CellPress

Trends in Biotechnology

Special issue: 40th anniversary

Review

Biosensors for healthcare: current and future perspectives

Eun Ryung Kim,[1,3] Cheulmin Joe,[1,3] Robert J. Mitchell,[2] and Man Bock Gu[1,*]

Biosensors are utilized in several different fields, including medicine, food, and the environment; in this review, we examine recent developments in biosensors for healthcare. These involve three distinct types of biosensor: biosensors for *in vitro* diagnosis with blood, saliva, or urine samples; continuous monitoring biosensors (CMBs); and wearable biosensors. Biosensors for *in vitro* diagnosis have seen a significant expansion recently, with newly reported clustered regularly interspaced short palindromic repeats (CRISPR)/Cas methodologies and improvements to many established integrated biosensor devices, including lateral flow assays (LFAs) and microfluidic/electrochemical paper-based analytical devices (μPADs/ePADs). We conclude with a discussion of two novel groups of biosensors that have drawn great attention recently, continuous monitoring and wearable biosensors, as well as with perspectives on the commercialization and future of biosensors.

Highlights

The capability and diversity of biosensors for human healthcare have grown tremendously, with novel approaches continually being developed.

Increased sensitivities of biosensors for *in vitro* diagnosis have been achieved using nanomaterials and nanotechnologies, while paper-based biosensor devices are a cost-effective alternative, all while maintaining high sensitivities and adapting ingenious design implementations.

While clustered regularly interspaced short palindromic repeats (CRISPR)-based biosensors have traditionally been used to detect nucleic acids, recent advances using bioreceptors have expanded their capabilities to non-nucleic acid targets.

Wearable biosensors now boast multiplex capabilities and are even battery-free and wireless.

Continuous monitoring and wearable biosensors are both considered to be key diagnostic tools for artificial intelligence-assisted human healthcare in the near future.

Biosensors: essential diagnostics for human healthcare

The coronavirus disease 2019 (COVID-19) pandemic has extensively exposed nonprofessionals to viral diagnostic technologies and terminologies, including PCR, real-time PCR, point-of-care technologies (POCTs), and LFAs. This has increased the public awareness of both biosensors (Box 1) and diagnostic technologies, as well as the global market size of this field, with the stock prices of related companies growing accordingly. Therefore, it is both timely and necessary to consider the whole biosensor picture, including their current status in human healthcare and future prospects. While biosensors have been implemented within diverse application fields, including bioprocesses for useful products, food and environmental safety, and national security; in this review, we focus solely on biosensors within human healthcare.

There are three distinct groups of biosensors essential for human healthcare (Figure 1, Key figure): *in vitro*, continuous monitoring, and **wearable** (see Glossary). Figure 2 presents an in-depth description of the biosensors discussed in this review, including their basic format (Box 1 and Figure 2A), biosensors for *in vitro* diagnosis (Figure 2B), and integrated biosensor devices (Figure 2C). It also highlights **CRISPR**-based biosensors (Figure 2D), continuous monitoring (Figure 2E), and wearable biosensors (Figure 2F). While other types of *in vitro* diagnostic biosensor are described in the literature, such as whole-cell biosensors, which are rarely utilized and limited for healthcare, the section discussing *in vitro* diagnostic biosensors focuses solely on those that provide high-level sensitivity and a strong possibility for commercialization, including antibody-, **aptamer**-, and nucleic acid-based biosensors, which are based on electrochemical, electrical, optical, or photoelectrochemical detection methods. In addition, the use of CRISPR-based biosensors as a class of *in vitro* diagnostic biosensors is specifically highlighted since the methodologies involved represent one of the hottest molecular diagnostic technologies being used currently to detect both nucleic acid and non-nucleic acid targets.

[1]Department of Biotechnology, Korea University, Anam-dong, Sungbuk-Gu, Seoul 02841, Republic of Korea
[2]Department of Biological Sciences, UNIST, Ulsan 44919, Republic of Korea
[3]These authors contributed equally to this work.

*Correspondence: mbgu@korea.ac.kr (M.B. Gu).

Box 1. Biosensors and their short history

According to the *Gold Book* of the International Union of Pure and Applied Chemistry (IUPAC), a biosensor 'is a device that uses specific biochemical reactions mediated by bioreceptors, such as isolated enzymes, immunosystems, tissues, organelles or whole cells, to detect chemical compounds, typically by electrical, thermal or optical signals' [1]. As such, all biosensors comprise two main components and their signals: bioreceptors and transducers, which generate a measurable signal when the bioreceptors and their targets interact (see Figure 2A in main text). The signals generated from the transducers are, in general, two types: signal-on and signal-off. Signal-on is a method in which the signal increases proportional to the quantity of the target detected, while the signal decreases in signal-off methods.

Leland C. Clark and Champ Lyons developed the first oxygen electrode in 1962 [2], followed by the first enzyme electrode developed by Updike and Hicks in 1967 [3]. By the late 1970s, only a handful of published papers were in the field of biosensors, including the invention of ion-selective field effective transistors, as well as the first microbe-based biosensors and the first immunosensors. The early 1980s saw a significant expansion in the biosensor field due to the development of the first fiber-optic biosensors and SPR biosensors, as well the use of novel bioreceptors, while the use of different bioreceptors within biosensors also saw their heyday during the early 1980s. However, aptamers were first implemented within bioassays during the late 1990s.

Shortly after IUPAC announced the formal definition of biosensors (in 1997), the first nanobiosensors were developed. These expanded the biosensor field by using a variety of different nanomaterials and nanotechnologies, including carbon nanotubes, quantum dots, NPs, nanocantilevers, nanowires, nanotubes, nano field effect transistors (nanoFET), and graphene.

In 2007, biosensors made the move to *in vivo* applications with the first implantable glucose biosensor, which ran successfully for 5 days. Several years later, in 2012, the first wearable biosensor was described, while the first CRISPR-based biosensor was developed in 2016. As hinted by the continual progression within this field, the definitions of both the field and the term 'biosensor' continue to evolve, and currently includes everything from biochips to DNA and protein chips to lab-on-a-chip (as integrated biosensor devices), from *in vitro* diagnostics to continuous monitoring and wearable or attachable sensors and, more recently, has expanded to embrace internet of things (IoT) and AI-based biosensors.

Biosensors for *in vitro* diagnosis

Biosensors for *in vitro* diagnosis have been extensively studied and developed for the detection of **miRNA**, protein biomarkers, and **circulating tumor cells (CTCs)** in biological samples, including blood, saliva, urine, and nose/throat swabs (Figure 2B). The commonly used **transducers** for these biosensors have typically been electrochemical or optical in nature. In this section, biosensors using these are reviewed, with an emphasis on both sensitivity improvement, a crucial factor in commercialization, as well as signal-on-type biosensors using sandwich-type simultaneous-binding pairs of **bioreceptors**. Table 1 summarizes each of these different methods along with their sensitivities and specific characteristics for comparison [4–57]. The different amplification protocols, combined with their respective transducers, offer sensitive detection of not only miRNAs, but also protein biomarkers and CTCs.

One main class of *in vitro* diagnostic biosensors is optical biosensors, of which **surface-enhanced Raman scattering (SERS)**-based biosensors, which use inelastic light scattering enhanced by nanoparticles (NPs) when adsorbed onto corrugated metal surfaces, are a major player. Therefore, it should come as no surprise that a crucial research focus in SERS-based biosensor development is the recruitment of different nanostructured materials, or their combinations, to enhance the Raman signals generated [17–21]. An example of a successful biosensor design is that reported by Lee *et al.* in which a plasmonic gold nanopillar with a head-flocked structure was used as a SERS substrate in a hybridization-based sandwich format to detect miRNAs, with a reported limit of detection (LOD) of 1 aM while also selectively distinguishing between single-base mismatched miRNAs [20].

Other optical biosensors use **surface plasmon resonance (SPR)** principles, and are divided into prism- and optical fiber-based platforms. SPR-based biosensors use the principle of

Glossary

Aptamers: single-stranded DNA or RNA (oligonucleotides), which bind to various targets forming 3D structures with high affinity and specificity.
Artificial intelligence (AI)-assisted biosensors: platforms that utilize AI in characterizing, classifying, and interpreting the signal generated. Implementation of AI processes into the biosensor helps address limitations in signal generation (e.g., signal:noise issues) and interpretation (false negative/positives and impacts of the environment on the interpretation).
Baseline drifts: classified as a type of long-term noise and defined as a change in the reference position caused by a shift in temperature, solvent, or both.
Biofuel cell: type of fuel cell using biocatalysts to convert biochemical energy to electrical energy.
Bioreceptors: molecules that specifically recognize analytes/targets. Antibodies, aptamers, and enzymes are examples of bioreceptors.
Circulating tumor cells (CTCs): rare type of cancer cell released from the (primary) tumor into the bloodstream.
Clustered regularly interspaced short palindromic repeats (CRISPR): CRISPR/Cas is a system that, during viral infection, stores a portion of viral DNA in the host cell genome, expresses CRISPR (cr)RNA from this stored DNA sequence, and binds to a specific CRISPR protein, which then destroys the viral nucleic acids.
Iontophoresis: technique using a direct current to introduce ionized substances (e.g., drugs) through intact skin.
miRNA: short (21–25 nucleotides) single-stranded RNA, stably present in plasma; cancer-specific biomarkers.
Reverse iontophoresis: technique by which molecules are removed from within the body for detection.
Self-monitoring of blood glucose (SMBG): technique in which patients with diabetes use a blood glucose reader to directly measure their blood sugar.
Specific high-sensitivity enzymatic reporter unlocking (SHERLOCK): CRISPR-based platform that uses Cas13a with collateral effect and isothermal amplification functions. It amplifies the guide RNA by RT-RPA and the activated CRISPR cleaves a

refractive index (RI) changes resulting when a target molecule binds the bioreceptor at a nanoscale metal surface, leading to a detectable change in the SPR angle proportional to the mass of the target bound. However, prism-based optical biosensors require numerous optical and mechanical components, which limits their performance in on-site diagnoses. In response, recent studies have leaned toward fiber-optic-SPR (FO-SPR)-based biosensors [42–45], with 2D nanomaterials [i.e., molybdenum disulfide (MoS_2) or MXene] used to expand the immobilization area and, consequently, increase target binding and improve sensitivity. One successful example of this is gold-coated fibers modified with MoS_2 nanosheets to increase their surface area and hydrophobicity, and facilitate antibody immobilization, resulting in a LOD for bovine serum albumin (BSA) of only 0.29 μg ml^{-1} [44].

However, among the different transducer systems, electrochemical biosensors have dominated the field of *in vitro* diagnosis of miRNAs, protein biomarkers, and CTCs due primarily to their quick responses and quantitative results, because these biosensors detect changes in electron transfer rates at the electrode when the target binds to the bioreceptor. Thus, the sensitivity of these devices can be improved by enhancing electron transfer rates at the electrodes by: (i) increasing the electrode surface area; (ii) accelerating the electrochemical redox reactions; or (iii) mimicking enzymatic activities, such as with peroxidase catalytic activities. One common method to achieve these is through the use of nanomaterials, which also help to solve key issues related to the detection of rare targets (e.g., miRNAs, protein biomarkers, and CTCs) in complex samples, such as blood, by allowing researchers to recognize these targets directly [25–31,34–38]. However, researchers are not limited to only one enhancement, as illustrated by a CA125 oncomarker biosensor using a chitosan-gold NP/multiwall carbon nanotube/graphene oxide (CS-AuNP/MWCNT/GO) platform to both increase the electrode surface area and accelerate the redox reaction [29]. Using the peroxidase-like function of CS-AuNP alongside the high surface area of the MWCNTs enhanced the electrochemical reaction and the antibody immobilization efficiencies, allowing CA125 to be detected at concentrations as low as 0.002 U ml^{-1}. Similarly, the LOD for cardiac troponin I (cTnI) was 7.5 pg ml^{-1} when hybrid nanozymes comprising Au@Pt nanozymes and Fe_3O_4 NPs were used together to amplify the electrochemical signal [37]. In addition to proteins, electrochemical biosensors have also been successful in detecting nucleic acids (RNA and DNA) when coupled with isothermal amplification or nuclease-based cycling amplification methods [4–6,14]. Once more, the sensitivity was improved when different nanomaterials were incorporated into the biosensor design [7–13,15].

Some of the studies mentioned in the preceding text focus on detecting CTCs in human blood samples. CTCs are key to cancer metastasis and, as such, are a major biomarker in cancer diagnoses. While biosensors using optical transducers to detect CTCs in the human blood samples are rare [57], similar to biosensors for miRNA and protein biomarkers, most are electrochemical in nature and use nanomaterials or other protocols for signal amplification [46–56]. One successful CTC aptasensor used CeO_2@Ir nanorods (Ce@IrNRs) to amplify the signal and had a reported sensitivity of a single CTC cell ml^{-1} [49]. This is an important scientific development because the densities of CTCs in the bloodstream are extremely low (i.e., a few CTCs among 5 billion erythrocytes and 10 million leukocytes [58]), and the analytical sample volumes are limited. Given that these challenges are being addressed via novel methods to isolate, enrich, and maintain the viabilities of CTCs, topics not directly related to biosensing and bioreporters, only studies that are clearly biosensor related are cited in Table 1.

Integrated biosensor devices: LFAs, LOCs, μPADs, and ePADs

Integrated biosensor devices offer the advantage that suspected symptoms can be tested in the field (e.g., at home) and are not restricted by location (such as needing to go to a hospital). This

fluorescently labeled RNA reporter to produce a single base mismatch-specific signal.

Surface-enhanced Raman scattering (SERS): Raman spectroscopic method that enhances Raman scattering efficiency by adsorbing materials on the rough metal surface.

Surface plasmon resonance (SPR): optical phenomenon that occurs when plane-polarized light hits a thin metal film with refractive index changes; used to monitor binding interactions.

***Trans*-cleavage activities:** alternative activity of several Cas proteins that degrade nonspecific nucleic acids.

Transducer: device that converts biorecognition events to measurable signals, such as electrochemical, fluorescent, or colorimetric signals.

Wearable biosensor: device that can be attached to, or inserted into, a person's body to detect biofluids through the use of bioreceptors.

Key figure

Three distinct types of health-related biosensor based on their use in *in vitro* sampling (blood, saliva, urine, etc.), continuous monitoring, and wearable sensing

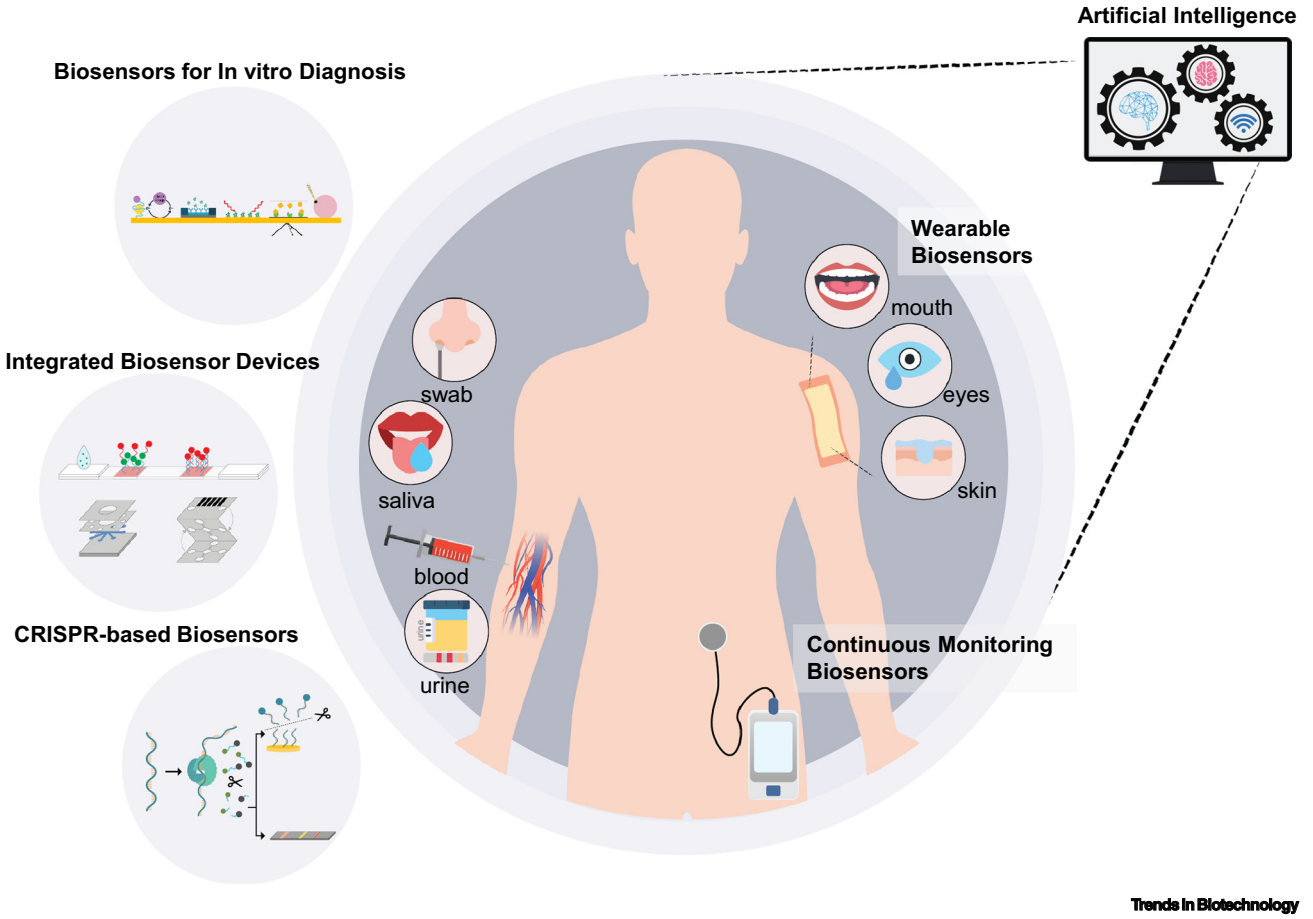

Figure 1. The conceptual implementation of artificial intelligence (AI) to oversee and interpret the data obtained is also depicted. Created with BioRender (BioRender.com).

allows nonexperts to predict the presence (or absence) of a disease or medical status with a simple measurement. On the whole, integrated biosensor devices, which combine the biosensor platform with fluidic channels for sample and buffer flow, should have several key qualities (e.g., affordability, sensitivity, specificity, user-friendliness, rapidity/robustness, deliverability, and require no equipment). Examples of successful devices include LFA devices, lab-on-a-chip (LOC), μPADs, and ePADs (Figure 2C).

One of the most commonly used integrated biosensor devices is LFAs. Used initially in pregnancy tests [59], LFAs utilize sandwich-type binding platforms to detect target biomarkers alongside an internal control to confirm that the test is working properly. Due in part to their simple design, LFAs have been widely adapted to a variety of biomarkers using antibodies (or, more recently, aptamers [60–62]) as receptors (Table 2 [60–91]). Many studies have considered using alternative signaling probes, such as AuNPs to fluorescent materials to SERS nanotags [65–70], to improve sensitivity, but these require

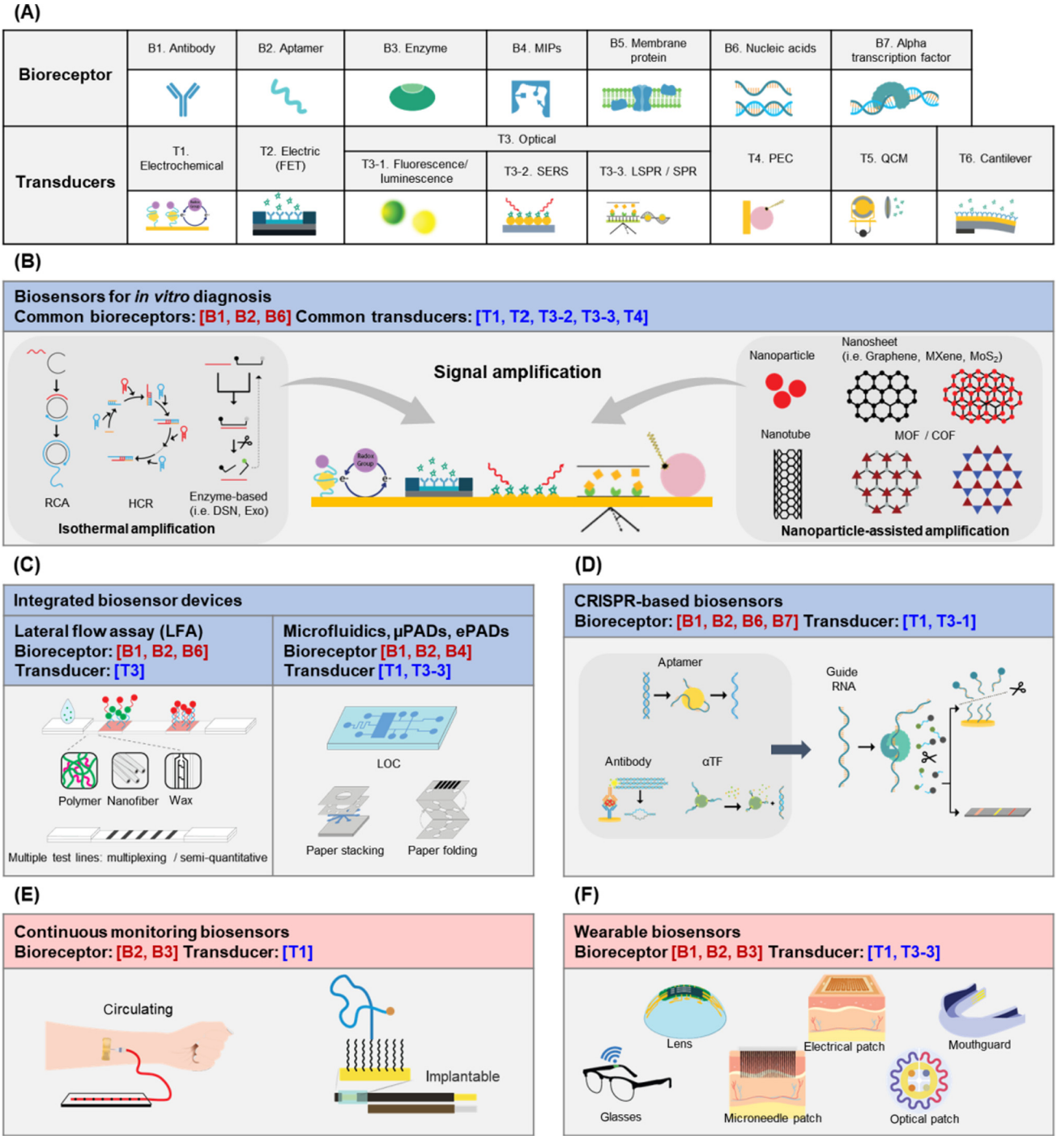

Figure 2. Key types of health-related biosensor. (A) Core components within biosensors, that is, the bioreceptors [antibody, aptamer, enzyme, molecular imprinted polymer (MIP), membrane protein, nucleic acid, and α transcription factor] and transducers [electrochemical, electric-field effect transistor (FET), fluorescence or luminescence, surface-enhanced Raman scattering (SERS), localized surface plasmon resonance (LSPR)/SPR, photoelectrochemical (PEC), quartz crystal microbalance (QCM), or cantilever), which can be combined to form specific biosensors. (B) Biosensors for *in vitro* diagnoses, showing the various methodologies used to amplify the signals and improve sensitivities for miRNA, for protein biomarkers, and for circulating tumor cells (CTCs) in blood. This can be achieved through the use

(Figure legend continued at the bottom of the next page.)

external fluorescence or SERS readout devices, limiting their portability. Another approach to enhance the sensitivity has been to add barrier systems (automated) for fluid flow control on the membranes, whereby hydrophobic/soluble barriers act to delay fluid flow rates within the LFAs. This both increases reaction times between the receptors and their targets and leads to improved sensitivities (Table 2). Interestingly, by coupling a water-soluble polymer barrier, polyvinyl alcohol (PVA) with Au-ion catalytic amplification, one group achieved a 543-fold enhanced sensitivity for cTnI over a commercial LFA [75]. Another improvement in LFAs being explored is the development of portable readers that provide semiquantification along multiple test lines, or even quantification with smartphone-based readers [75,76], progress that expands these assays from a simple 'Yes/No' format.

While LFAs are limited to 1D horizontal fluidic flow, microfluidic-based devices use patterned surfaces to create channels in which fluids can flow in different directions without the need for additional elements (i.e., conjugate pads or control lines) [77–79]. However, typical microfluidic devices are constructed of silicon, glass, and poly(dimethylsiloxane) (PDMS), and require pumps. With the development of the first paper-based μPAD in 2007 [92], followed by ePAD in 2009 [93], interest in these devices grew rapidly owing to their easy fabrication, use of printing or photolithography methods, and their use of paper, an inexpensive, disposable, and flexible material. Initially, μPAD and ePAD devices used a 2D design with multiple horizontal capillary flow for simultaneous multiplexed detection but were expanded into 3D folding, stacking, and sliding structures to allow samples to flow vertically with multilayer connections, enabling sandwich-type detection in paper-based devices [80–82,85–91]. While these devices may be cheap due to the use of paper, this does not necessarily come at the cost of sensitivity. For example, the 3D origami paper-based analytical device (3D-soPAD) is capable of detecting human immunoglobulin G (HIgG) at concentrations as low as 0.01 ng ml^{-1} [80], while an ePAD comprising folded working-, counter-, and closing-layers detected severe acute respiratory syndrome coronavirus 2 (SARS-CoV-2) IgG, IgM, and spike proteins with LODs of 0.96, 0.14, and 0.11 ng ml^{-1}, respectively [89]. Table 2 summarizes different integrated biosensor devices and their specific features/characteristics. However, while some modifications offer versatility, enhancing the sensitivity and reproducibility of these devices remain hurdles due to the nature of paper and its fibers. As such, room to improve paper-based biosensors still exists.

CRISPR-based biosensors

The CRISPR-based biosensors combine the principles of CRISPR/Cas systems and their ***trans*-cleavage activities** (collateral cleavage activities) with bioreceptors. The first diagnostic application of CRISPR was in the detection of Zika virus [94], while more recent iterations seek to simplify the assay, as well as increase its detection speed and affordability (Table 3 [94–111]). For instance, when combined with microfluidic systems, CRISPR-based electrochemical biosensors are very effective, such as when combined with glucose oxidase (GOx)-modified antibodies for the efficient detection of miRNAs [98].

CRISPR-based biosensors to detect target molecules other than nucleic acids, including proteins and small molecules, have also been developed by combining them with other bioreceptors, such

of either isothermal amplification or nanoparticle (NP)-assisted amplification, as presented here. For instance, with isothermal amplification, the hybridization chain reaction (HCR) and rolling circle amplification (RCA) can be combined with electrochemical transducers to enhance their sensitivities to nucleic acids and CTCs, respectively. In addition, different nanomaterials, including carbon nanotubes, can be used to increase both the surface area of the electrodes and the number of bioreceptors that are immobilized. When combined with electrochemical transducers, these improvements enhance the detection of protein biomarkers. (C) Integrated biosensor devices, including lateral flow assays (LFAs), microfluidics, paper-based microfluidic analytical devices (μPADs), and electrochemical (e)PADs, respectively. (D) Clustered regularly interspaced short palindromic repeats (CRISPR)-based biosensors. Once the target is added, bioreceptors bind the target and activate the CRISPR/Cas system with its guide RNA, resulting in a signal generation either on electrochemical transducers or within integrated biosensor devices. (E) Continuous monitoring biosensors. (F) Wearable biosensors for different body fluids, including sweat, interstitial fluids, tears, and saliva, which are sampled from the skin, eyes, and/or mouth. Abbreviations: COF, covalent organic framework; DSN, duplex specific nuclease; Exo, exonuclease; LOC, lab-on-a-chip; MOF, metal organic framework.

Table 1. *In vitro* diagnostic biosensors for the detection of miRNA, protein biomarkers, and CTCs[a]

Transducer		Target	Bioreceptor type and signal (on/off)	Electrode (electrochemical) [b]	Signal amplification	LOD	Refs
miRNAs							
Electrochemical	DPV	miRNA-25	On	Y-shaped DNA nanostructure on GE	Nonlinear HCR	0.3334 fM	[4]
		miRNA-21	On	Hairpin DNA on GE	Bipedal DNA walkers and LNA-modified toehold mediated strand displacement reaction (TMSDR)	67 aM	[5]
		miRNA-196a	On	3′-PO_4-terminated CP on GE	DSN-based cyclic enzymatic signal amplification (CESA) and template-free DNA extension reaction	15 aM	[6]
		miRNA-21	Off	Nitrogen-doped functionalized graphene (NFG)/AgNPs/polyaniline (PANI) and complementary ssDNA on fluorine doped tin oxide (FTO) electrode	N/A	0.2 fM	[7]
			On	Polypyrrole-coated gold NP superlattice (AuNS) and ssRNA CP on GCE	N/A	78 aM	[8]
		miRNA let-7a, miRNA-21	On	N/A	Porous UIO-66-NH_2 MOF as nanocontainer to load electroactive dye (MB@UIO and TMB@UIO)	(let-7a) 3.6 fM (miR-21) 8.2 fM	[9]
		hsa-miR-486-5p	Off	Laser-induced self-N-doped porous graphene (LIG) as electrode	N/A	10 fM	[10]
		miRNA let-7a	Off	N/A	2D MnO_2 nanoflakes as nanozyme	0.25 nM	[11]
	SWV	miRNA-21	Off	Magnetically collected gold-coated MNPs on gold electrode	N/A	10 aM	[12]
		miRNA-21, miRNA-155	On	DNA circle capture probe with multiple target recognition domains anchored at tetrahedron DNA nanostructure (TDN) on GCE	N/A	(miR-21) 18.9 aM (miR-155) 39.6 aM	[13]
Photoelectrochemical		miRNA-155	On	N/A	T7 Exo-assisted target recycling amplification	27 aM	[14]
			Off	AuNPs/MoS_2/anodic aluminum oxide (AAO) as working electrode with excellent photoelectric conversion efficiency	N/A	3 aM	[15]
Electric	FET	miRNA let-7b	On		Bent (crumpled) graphene and peptide nucleic acid (PNA) probe	600 zM	[16]

Table 1. (continued)

Transducer		Target	Bioreceptor type and signal (on/off)	Electrode (electrochemical) [b]	Signal amplification	LOD	Refs
Optical	SERS	miR-133a	On		Hollow Au/Ag nanosphere as SERS tag and target-catalyzed hairpin assembly (CHA)	0.306 fM	[17]
		miRNA-21	On		Au@R6G@AgAu NPs (ARANPs) as SERS tag and DSN-assisted target recycling amplification	5 fM	[18]
		miRNA-10b	Off		Fe_3O_4@Ag as SERS tag and DSN-assisted target recycling amplification	1 aM	[19]
		miRNA-21, miRNA-222, miR-200c	On		Plasmonic gold nanopillars as SERS substrate and sandwich detection with two LNA probes	1 aM	[20]
		miRNA-182	Off		MXene/MoS_2@AuNPs as hot spots	6.61 aM	[21]
	Electrochemical SERS	miRNA-155	On	AuNP-electrodeposited indium tin oxide (ITO)-coated substrate	AuNP-packaging RNA three-way-junction (pRNA 3WJ) monoconjugate	60 aM	[22]
	SPR	miRNA-21	On		Gold nanorod (AuNR) and 2D antiomonene nanosheet	10 aM	[23]
	LSPR	miRNA-21	On		Au@Ag core–shell nanocube (Au@Ag NC) modified with tetrahedron-structured DNA (tsDNA)	0.1 aM	[24]
Protein biomarkers							
Electrochemical	CA	cTnI	Sandwich Ab (on)	AuNP on GCE	Trimetallic CuPtRh cubic nanobox embedded in amino group functionalized few-layer ultrathin ammoniated MXene (CuPtRh CNBs/NH_2-Ti_3C_2)	8.3 fg ml^{-1}	[25]
		CEA	Sandwich Ab (on)	AuNP on GCE	Microporous carbon sphere-loading AgNP-spaced Hemin/rGO	6.7 fg ml^{-1}	[26]
		PSA	Sandwich Ab (on)	AuNP functionalized nitrogen-doped graphene quantum dots (Au@N-GQDs) on GCE	Au@Ag core-shell NP-cuprous oxide (Cu_2O)	0.003 pg ml^{-1}	[27]
		Thrombin	Sandwich Apt (on)	Au-COF nanosheets on GCE	Au@ZIF-8(NiPd) rhombic dodecahedra	15 fM	[28]
		CA125	Sandwich Ab (on)	Chitosan-AuNP/ MWCNT/GO on GCE	AuNP-lactate oxidase (LOx)	0.002 U ml^{-1}	[29]
		cTnI	Sandwich Ab (on)	AuNP-loaded 2D MOF (Co-BDC)/MoS_2 on GCE	Dendritic platinum-copper alloy NPs (DPCN)-loaded MoS_2 nanosheet	3.02 fg ml^{-1}	[30]

(continued on next page)

Table 1. (continued)

Transducer		Target	Bioreceptor type and signal (on/off)	Electrode (electrochemical) [b]	Signal amplification	LOD	Refs
		Vaspin	Sandwich Apt (on)	Coccolith on SPGE	N/A	298 pM	[31]
		Staphylococcus aureus	Sandwich Apt (on)	N/A	N/A	39 CFU ml^{-1}	[32]
		ODAM	Sandwich Apt (on)	N/A	N/A	0.02 nM	[33]
	DPV	cTnI	Sandwich Ab (on)	Gold nanocube-functionalized GO (AuNC/GO) on GCE	Bimetallic gold/silver core-shell NC and nitrogen sulfur co-doped rGO (Au@AgNC/N,S-rGO)	33 fg ml^{-1}	[34]
		Galectin-3	Sandwich Ab (on)	N-doped graphene nanoribbons (N-GNR)-Fe-MOFs@AuNPs) on GCE	AuPt-MB nanohybrid	33.33 fg ml^{-1}	[35]
		MPT64 antigen	Sandwich Apt (on)	Polyethyleneimine (PEI)-Fe-MOF (P-MOF) with bimetallic core-shell Au@Pt NPs on GCE	AuNP-fullerene NPs (C_{60}NPs)-N-CNTs/GO	0.33 fg ml^{-1}	[36]
		cTnI	Sandwich Apt (on)	DNA nanotetrahedron (NTH) on SPGE	Fe_3O_4/PDDA/Au@Pt NPs	7.5 pg ml^{-1}	[37]
	SWV	cTnI	Sandwich Ab (on)	Titanium dioxide NP (TiO_2)-polypyrrole (PPy)-AuNP on GCE	AuNP-doped COFs and toluidine blue (TB-Au-COF)	0.17 pg ml^{-1}	[38]
Photoelectrochemical		CEA	Single Apt (on)	N/A	ZIF-8-assisted NaYF4: Yb,Tm@ZnO upconverter	0.032 ng ml^{-1}	[39]
Optical	LSPR	Amyloid beta (Aβ) 1–40, Aβ 1–42, and τ (tau) protein	Single Ab (on)		Rayleigh scattering peak shift of three different shapes of AuNPs: spheres (diameter, 50 nm), short rods (aspect ratio, 1.6) and long rods (aspect ratio, 3.6)	(1–40) 34.9 fM, (1–42) 26 fM, (τ) 23.6 fM	[40]
		τ protein	Single Ab (on)		Rayleigh scattering peak shift of immunogold shaped as a long rod (aspect ratio, 3.67) with addition of guanidine hydrochloride (Gua-HCl) as chaotropic agent to improve sensitivity	1 pM	[41]
	SPR	CEA	Sandwich Ab (on)		Ti_3C_2 MXene/AuNP composite for primary antibody and MWCNT-polydopamine (PDA)-AgNPs for secondary antibody	0.07 fM	[42]
	FO-SPR	IgG	Single Ab (on)		SnO_2-coated lossy mode resonance (LMR) D-shaped single-mode fibers (SMFs)	1 fM	[43]

Table 1. (continued)

Transducer		Target	Bioreceptor type and signal (on/off)	Electrode (electrochemical) [b]	Signal amplification	LOD	Refs
		BSA	Single Ab (on)		Gold-coated fiber modified with MoS_2 nanosheets for immobilization of antibodies	0.29 μg ml^{-1}	[44]
		CD44 protein	Single Ab (on)		Silanized ball resonator	107 ag ml^{-1} (4.7 aM)	[45]
CTCs							
Electrochemical	DPV	MCF-7	Sandwich Apt (on)	MWCNT/poly(glutamic acid) (PGA) on GCE	AgNP labeling	25 cells ml^{-1}	[46]
			Sandwich Ab (on)	AuNPs/acetylene black (AuNPs/AB) on electrode	Pt@Ag nanoflowers (Pt@AgNFs) labeling	3 cells ml^{-1}	[47]
		HepG2	Single Apt (off)	DNA tetrahedral nanostructure on SPGE	Rolling circle amplification (RCA)-coupled duplex/hemin DNAzyme amplification	3 cells ml^{-1}	[48]
		MCF-7	Sandwich Apt (on)	N/A	CeO_2@Ir nanorods and enzyme-free DNA walker	1 cell ml^{-1}	[49]
		HeLa	Sandwich Apt (on)	N/A	Tyramide signal amplification (TSA) with PtNPs@HRP@aptamer as catalytic probe and tyramine-functionalized infinite coordination polymer (ICPs@Tyr) as electroactive signal tag	2 cells ml^{-1}	[50]
	LSV	MCF-7	Sandwich Apt-Ab (on)	N/A	DNA-templated silver nanoclusters (DNA-AgNCs)	3 cells ml^{-1}	[51]
	Amperometry	MCF-7	Sandwich Ab-Apt (on)	DNA primer and circular template complexes immobilized SPGE for RCA	Multivalent-aptamer network	5 cells ml^{-1}	[52]
	SWV	Ramos and CCRF-CEM	Sandwich Apt (on)	Magnetically separated Apt-functionalized and AuNP array-decorated magnetic graphene nanosheet (AuNPs-Fe_3O_4-GS) on screen-printed carbon electrode (SPCE)	Electroactive species-loaded AuNP probes	(Ramos) 4 cells ml^{-1} (CCRF-CEM) 3 cells ml^{-1}	[53]
		MCF-7	Sandwich Ab-Apt (on)	N/A	RCA	1 cell ml^{-1}	[54]
PEC		MCF-7	Sandwich Ab-Apt (off)	Hexagonal carbon nitride tubes (HCNTs) on GCE	Cu_2O NP labeling	1 cell ml^{-1}	[55]
Direct plasmon-enhanced electrochemistry		CCRF-CEM and MCF-7	Single apt (off)	Gold nanostar-modified glassy carbon electrode	N/A	(CCRF-CEM) 5 cells ml^{-1} (MCF-7) 10 cells ml^{-1}	[56]
Optical	FO-SPR	MDA-MB-415	Single Apt (on)		AuNP coating onto optical fiber (tilted fiber Bragg grating)	10 cells ml^{-1}	[57]

as antibodies, enzymes, aptamers, and allosteric transcription factors (αTFs) (Table 3). In such cases, the role of the CRISPR system is as the primary reporter or signal amplifier, according to the bioreceptors used in the biosensor. For example, within conventional ELISAs, alongside antibodies, CRISPR replaced the enzymatic role in signal amplification in a process termed CLISA [100] and was adapted further alongside DNA (aptamer)-AuNPs, leading to nano-CLISA [101]. Aptamers, which are single-stranded nucleic acids, are preferred among the various bioreceptors because they are particularly easy to apply, given that CRISPR-Cas systems recognize nucleic acids [102–109]. As such, when combined with aptamers, DNA-locking systems via hybridization are common adaptations within CRISPR-based biosensors (Table 3). In the presence of a target molecule, the aptamer releases a DNA lock and activates CRISPR, leading to cleavage of a reporter sequence and production of a measurable fluorescence, luminescence, and electrochemical signal. Another adaptation was seen in the **specific high-sensitivity enzymatic reporter unlocking (SHERLOCK)**-based profiling of *in vitro* transcription (SPRINT) biosensor, which recognizes transcriptional effector molecules, including metal ions and antibiotics [110,111].

Table 3 highlights recent trends in CRISPR-based biosensors. Although these biosensors are extremely effective in nucleic acid analyses, their use in the detection of non-nucleic acid targets is still at an early stage. However, this is expected to change given that CRISPR-based systems are coupled more often with aptamers [i.e., single-stranded (ss)RNA or ssDNA] that can hybridize the CRISPR/Cas guide RNA as well as act as bioreceptors themselves, a marriage of sorts that is leading to improved sensitivities with these devices.

Continuous monitoring biosensors

While the **self-monitoring of blood glucose (SMBG)** biosensor is the most widely used system, it only displays the blood glucose level at a specific time point and does not show long-term trends. In response, the first continuous-monitoring platform, the FDA-approved Medtronic MiniMed Gold, is an electrochemical-type glucose sensor that uses an enzyme (i.e., GOx) to measure blood glucose levels every 10 s over a 3-day period, but does not display the data in real time [112].

Recently, continuous glucose monitoring (CGM) has shifted away from SMBGs, with research focusing primarily on enzyme-based minimal or non-invasive electrochemical wearable sensors to sense glucose in the patient's interstitial fluids (ISFs), sweat, and saliva. One example is the microneedle-based self-powered **biofuel cell** sensor used to detect glucose in artificial ISF [113], which was developed further into a CGM biosensor that enabled insulin delivery via a closed-loop specific pancreas system over a 5-day period [114]. Non-invasive methods have also been explored, including a patch-type skin-attached electrode that extracts glucose from the ISF through **reverse iontophoresis** [115,116] or, in combination with sweat stimulation using pilocarpine, to simultaneously monitor for glucose in the ISF and alcohol in the sweat [116]. While each of the aforementioned biosensors used enzymes as their transducing elements, a revolutionary method was reported in 2010 where abiotic glucose-responsive fluorescent monomers were developed and applied subdermally to measure glucose within a live animal

Notes to Table 1:
[a]Abbreviations: Ab, antibody; AgNP, silver nanoparticle; Apt, aptamer; bBSA, biotinylated bovine serum albumin; CA, chronoamperometry; CA125, carcinoma antigen 125; CEA, carcinoembryonic antigen; COF, covalent organic framework; CP, capture probe; CRP, human C-reactive protein; cTnI, cardiac troponin I; DPV, differential pulse voltammetry; DSN, duplex-specific nuclease; GCE, glassy carbon electrode; GE, gold electrode; HCR, hybridization chain reaction; IgG, immunoglobulin G; LNA, locked nucleic acid; LOD, limit of detection; LSPR, localized surface plasmon resonance; LSV, linear sweep voltammetry; MB, methylene blue; MNP, magnetic nanoparticle; MOF, metal organic framework; MWCNT, multiwalled carbon nanotube; NC, nanocube; NP, nanoparticle; ODAM, human odontogenic ameloblast-associated protein; PDDA, poly (diallyldimethylammonium chloride); PSA, prostate-specific antigen; SPGE, screen-printed gold electrode; ss, single-stranded; SWV, square wave voltammetry; TMB, 3,3′,5,5′-tetramethylbenzidine; Vaspin, visceral adipose tissue-derived serpin; ZIF, Zeolitic Imidazolate Framework.
[b]Electrode modification for electrochemical or photoelectrochemical biosensor.

Table 2. Specific features and characteristics of integrated biosensor devices[a]

Flow direction	Sample		Detection				Features	Refs
	Target	Volume (μl)	Bioreceptor	Assay time (min)	LOD	Signal amplification strategy		
LFA								
Dipstick	Vaspin	50	Sandwich Apt	N/A	0.137 nM (buffer) 0.105 nM (serum)	N/A		[60]
	H5N2 virus	50	Sandwich Apt	N/A	1.27×10^5 EID_{50} ml^{-1} (buffer) 2.09×10^5 EID_{50} ml^{-1} (duck's feces)	N/A		[61]
	ODAM	5	Sandwich Apt	N/A	0.24 nM (buffer) 1.63 nM (saliva)	N/A		[62]
	IgG	70	Sandwich Ab	20	14.47 ng ml^{-1}	Dissoluble wax barrier with on membrane resulted in 12 min delayed and 51.7-fold enhanced sensitivity compared with unmodified LFA		[63]
	HIV p24 antigen	50	Nanobody-Ab	20	0.8 pg ml^{-1} (32.5 fM) (human serum)	Catalytic amplification of Au-Pt core-shell nanocatalysts (PtNCs) resulted in 100 times lower detection limit		[64]
Horizontal	H-FABP	75	Sandwich Ab	10	0.21 ng ml^{-1}	Quantum dots as signaling probe	Quantification with smartphone	[65]
	HIV-1 RNA	5	Nucleic acid	N/A	820 zM	Fluorescent nanodiamond as signaling probe		[66]
	HIV-DNA	50	Nucleic acid	10–15	0.76 pM	Quantum dots as signaling probe and strand displacement amplification (SDA) before loading		[67]
	hCG	N/A	Sandwich Ab	N/A	1.6 mIU ml^{-1}	SERS nanotag as signaling probe	Scanning signal within 5 s	[68]
	Influenza A H_1N_1 virus and human adenovirus	70	Sandwich Ab	30	(H_1N_1) 50 pfu ml^{-1} (HAdV) 10 pfu ml^{-1}	SERS nanotag (Fe_3O_4@Ag NPs) as signaling probe	Magnetic property of NPs for separation of analytes from sample solution	[69]
	Three cardiac biomarkers (Myo, cTnI, and CK-MB)	100	Sandwich Ab	7	(Myo) 1 ng ml^{-1} (cTnI) 0.8 ng ml^{-1} (CK-MB) 0.7 ng ml^{-1}	SERS nanotag (Ag^{NBA}@Au) as signaling probe	Three test lines for multiplexing	[70]
	Human IgG	200	Sandwich Ab	15	8 ng ml^{-1}	Wax pillar as barrier on membrane led to threefold improved detection compared with barrier-free LFA	Different pattern was tested	[71]
	Alpha-fetoprotein (AFP)	100	Sandwich Ab	10	1 ng ml^{-1} (by naked eye) 0.1 ng ml^{-1} (quantitative result by phone)	Wax printed with pattern on membrane led to 11 s delayed compared with no-delayed LFA	Quantification with smartphone and alkaline phosphatase (ALP)-conjugated secondary antibody for signal generation	[72]

(continued on next page)

Table 2. (continued)

Flow direction	Sample		Detection				Features	Refs
	Target	Volume (μl)	Bioreceptor	Assay time (min)	LOD	Signal amplification strategy		
	Dengue virus RNA	50	Nucleic acid	60	~100 copies	3% agarose with glass fiber led to 178.73 ± 0.54 s delayed and tenfold enhanced detection compared with unmodified LFA	Estimated cost (~US$1.344)	[73]
	TnI	120	Sandwich Ab	20	0.24 ng ml^{-1}	Silver-enhancement reagents ($AgNO_3$ and hydroquinone) encapsulated by water-soluble polymer [poly (ethylene oxide)] shell led to ten times enhanced detection compared with unmodified LFA		[74]
	cTnI	50	Sandwich Ab	20	0.92 ng ml^{-1}	Water-soluble polymer, polyvinyl alcohol and catalytic/colorimetric gold-ion amplification led to 543-fold enhanced detection compared with unmodified LFA	Quantification with smartphone reader	[75]
	Ebola virus IgG	20	Sandwich Ab	15	200 ng ml^{-1}	N/A	Quantification with smartphone reader	[76]
LOC								
Vertical	SARS-CoV-2 spike protein Ab	1000	Single Ab	30	0.08 ng ml^{-1} (0.5 pM) (with 1:1000 diluted human plasma)	Gold nanospike-covered substrate		[77]
Horizontal	SARS-CoV-2 Ab	15	Sandwich (antigen) Ab	120	(anti-N-SARS-CoV-2 Rabbit IgG) 0.8 ng ml^{-1}	Multiplexed electrochemical lab-on-a-chip device detected anti-SARS-CoV-2 immunoglobulins and SARS-CoV-2 RNA with Cas12a-based enzymatic cleavage		[78]
	SARS-CoV-2 spike S1 protein Ab and its RBD Ab	N/A	(SARS-CoV-2 antigen)	N/A	(S1 Ab) 2.8 fg (EIS) (RBD Ab) 16.9 fg (EIS)	3D-printed COVID-19 test chip (3DcC) with antigen-modified gold micropillars on electrode		[79]
μPAD								
Vertical	Protein A	221	Sandwich Ab	7	0.01 ng ml^{-1}	3D-soPAD with smartphone reader; AuNPs as carrier for signal amplification; Ab-HRP conjugates stored by freeze-drying in sugar matrices comprising 10% sucrose/10% trehalose (w/w %) for long-term storage		[80]
	CEA, AFP, and CA199	10	Sandwich Ab	5	(CEA) 0.03 ng ml^{-1} (AFP) 0.05 ng ml^{-1} (CA199) 0.09 ng ml^{-1} (human serum)	3D vertical-flow paper-based device (3VPD) with external device for fluorescence		[81]
	CRP	100	Sandwich Ab	30	1 ng ml^{-1}	Sliding strip for several steps		[82]

Table 2. (continued)

Flow direction	Sample		Detection				Features	Refs
	Target	Volume (μl)	Bioreceptor	Assay time (min)	LOD	Signal amplification strategy		
μPAD + LFA								
Vertical + horizontal	*Plasmodium falciparum* (causative agent of malaria)	40	Nucleic acid	50	10^4 IU ml^{-1}	Sample preparation including DNA extraction, LAMP isothermal amplification in μPADs, and detection of the DNA amplicons in LFA		[83]
ePAD								
Vertical	PSA	10	Single Apt	60	10 pg ml^{-1} (DPV)	AuNPs/rGO/thionine nanocomposite-modified electrode		[84]
	H_1N_1 virus	40	Sandwich Ab	6	4.7 PFU ml^{-1} (EIS) 2.27 PFU ml^{-1} (optical) (saliva)	Sample pad comprised two different pore size (DP) papers for filtration and flow control, optical signal from unbound secondar Ab-HRP		[85]
	miRNA-21	10	Nucleic acid	N/A	0.434 fg (DPV) 7.382 fg (optical)	Signal amplification by cerium dioxide-Au@glucose oxidase (CeO_2-Au@GOx), electrochemical and colorimetric detection at the same time		[86]
	Ascorbic acid (AA), AFP, and serotonin (5-HT)	1	Single Ab	N/A	(AA) 92.8 uM (CA) (AFP) 0.63 ng ml^{-1} (EIS) (5-HT) 0.15 mM (DPV)	Sequential μPAD (sePAD) comprising two components, an origami folding paper (oPAD) and a movable reagent-stored pad (rPAD) with flow-through and stopped-flow		[87]
	Hepatitis B surface antigen (HbsAg) and hepatitis C core antigen (HCVcAg)	15	Single Ab	500 (s)	(HbsAg) 18.2 pg ml^{-1} (HCVcAg) 1.19 pg ml^{-1} (by CA)	Device with dual flow, fast-flow for automated washing of unbound antigens and delayed for storage of redox reagent		[88]
	SARS-CoV-2 spike protein Ab	10	(SARS-CoV-2 antigen)	30	1 ng ml^{-1} (SWV)	Paper-folded device comprising closing, counter, and working ePAD with smartphone reader, resulting in 1000 times more sensitive result than LFA		[89]
	CEA and NSE	20	Single Apt	60 <	(CEA) 2 pg ml^{-1} (DPV) (NSE) 10 pg ml^{-1} (DPV)	Graphene-thionine-AuNPs modified electrode for CEA and Prussian blue (PB)-PEDOT-AuNP-modified electrode of NSE to immobilize Apt		[90]
	CEA	5	MIPs	60	0.32 ng ml^{-1} (DPV)	GO-chitosan-modified electrode, movable valve for continuous fluid delivery and MIP formed by electropolymerization of dopamine		[91]

[a]Abbreviations: CA199, cancer antigen 199; CK-MB, creatine kinase-MB iso-enzymes; EIS, electrochemical impedance spectroscopy; hCG, human chorionic gonadotropin; H-FABP, heart-type fatty acid binding protein; LAMP, loop-mediated isothermal amplification; Myo, myoglobin; NSE, neuron-specific enolase; RBD, receptor-binding domain.

[117]. This led to commercialization of the FDA-approved Eversense system, a CGM that works stably for 90 days [118].

CMBs (Figure 2E) for targets other than blood glucose have also been developed, including devices to measure levodopa [119] and β-lactam antibiotics [120], both of which use enzymes (tyrosinase and β-lactamase, respectively). Aside from enzymes, the most common bioreceptor used in CMBs is aptamers. The first CMBs, which were not applied *in vivo*, used aptamers and binding-induced protein folding to sense antibiotics in microfluidic electrochemical sensor chips [121,122]. Implantable *in vivo* wire-type electrodes to monitor antibiotics in the blood plasma

Table 3. Recent progress in CRISPR-based biosensors and their application alongside other bioreceptors, including aptamers, antibodies, and αTFs[a]

Target	Bioreceptor	CRISPR-Cas system		Signal	LOD	Feature	Refs
		Enzyme	Amplification				
Zika RNA	Nucleic acid	Cas9	NASBA	Optical (colorimetric)	3 fM	NASBA-CRISPR cleavage leverages sequence-specific nuclease activity of CRISPR/Cas9 to discriminate between viral lineages	[94]
SARS-CoV-2 RNA (E and N genes)	Nucleic acid	Cas12a	Nucleic acid preamplification (RT-Lamp)	Optical (fluorescence)	10 copies μl^{-1}	DETECTR-based LFA	[95]
Listeria monocytogenes and African swine fever virus DNA	Nucleic acid	Cas9	Nucleic acid preamplification (PCR, RPA)	Optical (colorimetric)	200 copies	CASLFA	[96]
DNA/RNA (dengue, Zika virus)	Nucleic acid	Cas13, Cas12a, Csm6	Nucleic acid preamplification (RPA)	Optical (fluorescence)	< 2aM	SHERLOCK v2 integrated multiplexed LFA	[97]
RNA (miRNA)	Nucleic acid	Cas13a	Nucleic acid preamplification free	Electrochemical (amperometric)	2–18 pM	E-CRISPR	[98]
RNA (miRNA)	Nucleic acid	Cas13a	Nucleic acid preamplification free	Electrochemical (amperometric)	2–18 pM	E-CRISPR (multiplexing)	[99]
SARS-CoV-2 RNA	Nucleic acid	Cas12a	Nucleic acid preamplification (LAMP)	Electrochemical (cyclic voltametric)	0.8 copies μl^{-1}	Usage of polystreptavidin-HRP/-TMB-based reaction enables further amplification	[78]
Protein (IL-6, VEGF)	Antibody	Cas13a	Nucleic acid preamplification (T7 transcription amplification)	Optical immunoassay (fluorescence)	2.29 fM, 0.81fM, respectively	CLISA	[100]
Protein (CEA and PSA)	Antibody, aptamer	Cas12a	DNA-AuNPs	Optical immunoassay (fluorescence)	69.5 aM, 175 aM, respectively	Nano-CLISA	[101]
Toxin (deoxynivalenol)	Aptamer	Cas12a	CRISPR-based signal enhancement	Optical (luminescence)	0.64 ng ml^{-1}	Ti_3C_2Tx MXene-based luminescence resonance energy transfer	[102]
Small molecule (ATP)	Aptamer	Cas12a	CRISPR-based signal enhancement	Optical (fluorescence)	104 nM		[103]
Small molecule, metal ion (ATP, Na^+)	Aptamer. DNAzyme	Cas12a	CRISPR-based signal enhancement	Optical (fluorescence)	0.44 μM, 0.10 mM, respectively		[104]
Protein, small molecule (alpha fetoprotein, cocaine)	Aptamer	Cas12a	CRISPR-based signal enhancement	Optical (fluorescence)	0.07 fM, 0.34 μM, respectively	Plug-and-play design	[105]
Small molecule, metal ion (ATP and Na^+)	Aptamer	Cas12a	CRISPR-based signal enhancement	Optical (luminescence)	87 pM, 4.3 nM, respectively	Bead-supported upconversion LRET	[106]
Protein (TGFβ1)	Aptamer	Cas12a	CRISPR-based signal enhancement	Electrochemical (cyclic voltametric)	0.2 nM		[107]

Table 3. (continued)

Target	Bioreceptor	CRISPR-Cas system		Signal	LOD	Feature	Refs
		Enzyme	Amplification				
Protein (alpha-methylacyl-CoA racemase)	Aptamer	Cas12a	CRISPR-based signal enhancement	Electrochemical (electrochemiluminescence)	0.18 pM	Y-shaped DNA nanostructure assembled-spherical nucleic acids	[108]
Protein (vascular endothelial growth factor)	Aptamer	Cas12a	CRISPR-based signal enhancement	Electrochemical (SWV)	0.33 pM	'Signal on-off-super on' sandwich-type aptamer sensor	[109]
Nucleotides, metabolites of amino acids, tetracycline, and monatomic ions	αTF	Cas13a	CRISPR-based signal enhancement	Optical (fluorescence)	~ μM	SPRINT	[110]
Small molecules and double-stranded DNA	αTF	Cas12a	CRISPR-based signal enhancement	Optical (fluorescence)	~ μM	CaT-SMelor	[111]

[a]Abbreviations: αTF, allosteric transcription factor; CASLFA, CRISPR/Cas9-mediated lateral flow nucleic acid assay; CaT-SMelor, CRISPR-Cas12a- and αTF-mediated small-molecule detector); CLISA, CRISPR/Cas13a signal amplification linked immunosorbent assay; DETECTR, DNA endonuclease-targeted CRISPR trans reporter; E-CRISPR, CRISPR/Cas integrated electrochemical biosensors; NASBA, nucleic acid sequence-based amplification; RPA, recombinase polymerase amplification.

were also developed [123–125] but, unfortunately, **baseline drifts** due to adherence of blood cells to the electrodes were observed.

Subsequently, a patch biosensor, which can also be categorized as a wearable biosensor, was developed using three different aptamers to monitor for tobramycin, doxorubicin, and irinotecan, an antibiotic and two chemotherapeutic drugs, respectively, within the ISF via microneedles [126]. While another microfluidic chip-based biosensor used both an antibody and an aptamer for the continuous and simultaneous monitoring of glucose and insulin [127], antibodies, with their high binding affinities and slow dissociation rates, are rarely used within CMBs because the device needs to reset for continuous monitoring to be realized. Thus, aptamers are the preferred bioreceptors.

Wearable biosensors

Wearable sensors were initially seen as physical sensors to monitor temperature, calories, and heartbeat. Toward this end, flexible materials and electrodes were developed to ensure that essential bodily contact occurred and became the foundation for many electrochemical- and optical transducer-based wearable biosensors (Figure 2F). Samples that are not secreted outside the body, such as blood and ISF, could be targeted using microneedles. Such wearable devices have been developed to monitor alcohol [128], simultaneously detect lactate-glucose or alcohol-glucose [129], or detect tyrosinase, a cancer-related enzyme [130]. More recently, a biosensor that sensitively detects anti-SARS-CoV-2 IgM/IgG antibodies has also been reported [131].

However, samples secreted outside the body, such as sweat, tears, and saliva, can also be targeted with non-invasive wearable biosensors, most of which use enzymes as their bioreceptors. One such system, a GOx-based mouthguard biosensor, was developed to measure glucose concentrations within the saliva and transmit the data in real time via a Bluetooth link [132]. This was miniaturized within a tooth-mounted biosensor for glucose detection that used conformal radio frequency (RF) to transmit data in real time [133]. While successful, saliva-based biosensors are still in the early stages of development since target concentrations are typically lower in the saliva than in the blood or sweat, meaning false positives can be a problem.

Another medium for biosensing is tears. In fact, electrochemical wireless soft contact lenses that measure both the glucose concentration and intraocular pressure (IOP) [134], integrate glucose sensors, wireless power transfer circuits, and display pixels to visualize the signals in real time [135] and also monitor cholesterol [136], were all successfully developed. Optical monitoring biosensors based on contact lenses are also possible, including one device that swells slightly based on the glucose concentration and changes the diffractive light intensity sufficient for it to be measured using a smartphone [137]. Another optical contact lens biosensor detects two important biomarkers in eye-related diseases, metalloproteinase-9 (MMP-9) and the IOP, via SERS and color shifts, respectively [138]. One concern with contact lens-based systems is the possibility of infection, irritation, or vision impairment. In response, researchers have developed a unique eyeglasses-based biosensor that uses a microfluidic system to collect tear samples and monitor for glucose, alcohol, and vitamins [139].

Similarly, electrochemical tattoo-, bandage- and patch-type biosensors using enzymes to monitor sweat samples have been reported [140,141], with some evolving further to provide dual biofluid sampling (i.e., capable of detecting ISF and sweat biomarkers simultaneously via **iontophoresis** and reverse iontophoresis) [116,142,143]. Work has also enhanced their sensitivity, power efficiency, and versatility while reducing power consumption with chip-less electronic skins [144]. This led to a multiplexed patch-type colorimetric and electrochemical biosensor that combines microfluidics; in addition, integrated biofuel cell-based battery-free electrochemical detection platforms were developed for the detection of diverse physiological and physical targets (i.e., lactate, glucose, chloride, pH, and sweat rate/loss) [145–147]. Given that most wearable biosensors are built with enzyme-based electrochemical or optical sensors, target availability is limited. To overcome this problem, as well as enzyme stability issues, researchers successfully used $CoWO_4$ NPs (instead of GOx), reductive GO (rGO), and AuNP to detect ascorbic acid, lactate acid, creatinine, glucose, and hydrogen, all within a near-field communication (NFC)-based battery-less skin-interfaced platform [147].

Several devices were also fabricated that detect the hormone cortisol within sweat. Two such devices include a wearable lab-on-a-patch microfluidic device [148] and a battery-free biosensor that communicates with a smartphone via NFC chips [149]. While both devices use antibodies as their bioreceptors, the use of molecular-imprinted polymers or aptamers in wearable biosensors is also possible, with cortisol-targeting wearable aptasensors showing improved sensitivities [150,151]. Similarly, an IFNγ aptamer-based wearable device had a broad detection range (0.015–250 nM), low LOD (down to 740 fM), and was resilient, showing no visible damage and maintained a consistent response throughout regenerative (80 cycles) and crumpling (100 cycles) tests [152]. Finally, wireless multiplexed biosensors have also used both of these bioreceptors (i.e., enzymes and aptamers) to detect both glucose and serotonin [153].

While the above shows the tremendous progress made in the field of wearable biosensors, including multiplexing, alternate sampling sites, battery-free and wireless systems, at present, the commercialization of such devices remains limited due to a major challenge inherent to their nature, namely, accuracy, given that biomarker concentrations in the blood do not necessarily correlate with their concentrations in other bodily fluids, including sweat, tear, saliva, among others. However, as research into addressing this issue continues, commercialization should not be far off.

Concluding remarks and future perspectives

Since the introduction of the first glucose biosensor, biosensors for human healthcare have advanced tremendously, especially with the development of nanotechnology. While many

Outstanding questions

Can the signal-on method be implemented in μPADs in which simplicity (washing steps, running time, shorter protocols, etc.) is a virtue for field applications?

In continuous monitoring, the duration of the biosensor is a weakness due to enzyme activities decreasing while data errors increase with repeated usage. Can the duration of CMBs be extended?

Within CRISPR-based biosensors, new CRISPR enzymes are continuously being identified and developed, along with new nucleic acid diagnosis methodologies. For non-nucleic acid targets, CRISPR/Cas has so far been used to amplify the signal. Do other applications of CRISPR exist, other than signal amplification?

For wearable biosensors, the concentrations of the target (excluding glucose) in blood and other body fluids (excluding sweat) are not comparable. What can be done to ensure analytical reliability?

Can AI help to solve problems of reliability and accuracy and improve biosensor commercialization?

biosensors were highlighted in this review, we would be amiss not to mention that only a few of these have seen commercialization. To achieve this, as noted previously, many of the factors mentioned as desirable features of integrated biosensor devices need to be appraised. However, considering the platforms already commercially available, one key feature of most is the use of a 'sandwich-type biosensor' platform, in which two bioreceptors bind the target simultaneously, because this allows for very stable and sensitive signals to be generated, and can be coupled with other protocols to amplify the signal.

Similarly, each of the different platforms mentioned in this review has different strengths and weaknesses. For instance, integrated biosensor devices offer great portability, but many use single bioreceptors (aptamers or antibodies) and, thus, suffer low sensitivity. By contrast, fluorescence-based systems offer great sensitivity but require instrumentation, limiting their usefulness as an on-site diagnostic tool. Furthermore, owing to recent innovations in nanomaterials and nanotechnologies, electrochemical biosensors saw significant enhancements in their sensitivities for *in vitro* samples. In response, researchers have sought to expand the capabilities of the different platforms, such as through the use of flexible materials and electrodes within battery-free and wireless devices that, in conjunction with common smartphones, provide reliable data, which should guide these devices into the commercialization pipeline. This has led to an innovation within the biosensor field, namely, the prospective use of artificial intelligence (AI) in interpreting the signals generated by the devices (Figure 1) (see Outstanding questions).

Given the current state of continuous monitoring and the direction of wearable biosensor development, these **AI-assisted biosensors** can aid in every step of biosensing, from initial data analysis, via machine learning, to the integration of multiple biosensors and the identification of hidden biomarkers, marking AI as a key core advancement within the biosensor field in the coming years. In fact, AI has already aided single-receptor biosensors in several important ways, including raw data classification, anonymous detection, noise reduction, object identification, and pattern recognition [154–156]. Expanding these capabilities to multiplex biosensors will not only help generate (and interpret) large data sets, but also allow users to incorporate environmental factors and physical data acquired from wearable or CMBs in the analyses.

Acknowledgments

This work was supported by National Research Foundation of Korea (NRF) grants funded by the Korean Government (MSIT) (No. 2021R1A2C2013396 and No. 2020R1A2C2012158). This work was also supported by a Korea University Grant.

Declaration of interests

None are declared by the authors.

References

1. McNaught, A.D. and Wilkinson, A. (1997) *IUPAC. Compendium of Chemical Terminology* (2nd edn), Blackwell Scientific Publications
2. Clark, L.C. and Lyons, C. (1962) Electrode systems for continuous monitoring in cardiovascular surgery. *Ann. N. Y. Acad. Sci.* 102, 29–45
3. Updike, S.J. and Hicks, G.P. (1967) The enzyme electrode. *Nature* 214, 986–988
4. Zhou, L. *et al.* (2019) A label-free electrochemical biosensor for microRNAs detection based on DNA nanomaterial by coupling with Y-shaped DNA structure and non-linear hybridization chain reaction. *Biosens. Bioelectron.* 126, 657–663
5. Zhang, J. *et al.* (2018) A ratiometric electrochemical biosensor for the exosomal microRNAs detection based on bipedal DNA walkers propelled by locked nucleic acid modified toehold mediate strand displacement reaction. *Biosens. Bioelectron.* 102, 33–40
6. Guo, J. *et al.* (2018) An electrochemical biosensor for microRNA-196a detection based on cyclic enzymatic signal amplification and template-free DNA extension reaction with the adsorption of methylene blue. *Biosens. Bioelectron.* 105, 103–108
7. Salahandish, R. *et al.* (2018) Label-free ultrasensitive detection of breast cancer miRNA-21 biomarker employing electrochemical nano-genosensor based on sandwiched AgNPs in PANI and N-doped graphene. *Biosens. Bioelectron.* 120, 129–136
8. Tian, L. *et al.* (2018) Gold nanoparticles superlattices assembly for electrochemical biosensor detection of microRNA-21. *Biosens. Bioelectron.* 99, 564–570
9. Chang, J. *et al.* (2019) Nucleic acid-functionalized metal–organic framework-based homogeneous electrochemical biosensor for simultaneous detection of multiple tumor biomarkers. *Anal. Chem.* 91, 3604–3610

10. Wan, Z. *et al.* (2020) Laser induced self-N-doped porous graphene as an electrochemical biosensor for femtomolar miRNA detection. *Carbon* 163, 385–394
11. Wu, J. *et al.* (2021) Label-free homogeneous electrochemical detection of microRNA based on target-induced anti-shielding against the catalytic activity of two-dimension nanozyme. *Biosens. Bioelectron.* 171, 112707
12. Tavallaie, R. *et al.* (2018) Nucleic acid hybridization on an electrically reconfigurable network of gold-coated magnetic nanoparticles enables microRNA detection in blood. *Nat. Nanotechnol.* 13, 1066–1071
13. Xu, S. *et al.* (2020) One DNA circle capture probe with multiple target recognition domains for simultaneous electrochemical detection of miRNA-21 and miRNA-155. *Biosens. Bioelectron.* 149, 111848
14. Hou, T. *et al.* (2018) Truly immobilization-free diffusivity-mediated photoelectrochemical biosensing strategy for facile and highly sensitive microRNA assay. *Anal. Chem.* 90, 9591–9597
15. Jiao, S. *et al.* (2020) A novel biosensor based on molybdenum disulfide (MoS_2) modified porous anodic aluminum oxide nanochannels for ultrasensitive microRNA-155 detection. *Small* 16, 2001223
16. Hwang, M.T. *et al.* (2020) Ultrasensitive detection of nucleic acids using deformed graphene channel field effect biosensors. *Nat. Commun.* 11, 1543
17. Sun, Y. and Li, T. (2018) Composition-tunable hollow Au/Ag SERS nanoprobes coupled with target-catalyzed hairpin assembly for triple-amplification detection of miRNA. *Anal. Chem.* 90, 11614–11621
18. Ma, D. *et al.* (2018) Quantitative detection of exosomal microRNA extracted from human blood based on surface-enhanced Raman scattering. *Biosens. Bioelectron.* 101, 167–173
19. Pang, Y. *et al.* (2019) Dual-SERS biosensor for one-step detection of microRNAs in exosome and residual plasma of blood samples for diagnosing pancreatic cancer. *Biosens. Bioelectron.* 130, 204–213
20. Lee, J.U. *et al.* (2019) Quantitative and specific detection of exosomal miRNAs for accurate diagnosis of breast cancer using a surface-enhanced Raman scattering sensor based on plasmonic head-flocked gold nanopillars. *Small* 15, 1804968
21. Liu, L. *et al.* (2020) Ultrasensitive SERS detection of cancer-related miRNA-182 by MXene/MoS2@AuNPs with controllable morphology and optimized self-internal standards. *Adv. Opt. Mater.* 8, 2001214
22. Lee, T. *et al.* (2020) Single functionalized pRNA/gold nanoparticle for ultrasensitive microRNA detection using electrochemical surface-enhanced Raman spectroscopy. *Adv. Sci.* 7, 1902477
23. Xue, T. *et al.* (2019) Ultrasensitive detection of miRNA with an antimonene-based surface plasmon resonance sensor. *Nat. Commun.* 10, 28
24. Zhang, Y. *et al.* (2018) Single-molecule analysis of microRNA and logic operations using a smart plasmonic nanobiosensor. *J. Am. Chem. Soc.* 140, 3988–3993
25. Dong, H. *et al.* (2020) A signal amplification strategy of CuPtRh CNB-embedded ammoniated Ti3C2 MXene for detecting cardiac troponin I by a sandwich-type electrochemical immunosensor. *ACS Appl. Bio. Mater.* 3, 377–384
26. Zhang, C. *et al.* (2019) Sandwich-type electrochemical immunosensor for sensitive detection of CEA based on the enhanced effects of Ag NPs@CS spaced Hemin/rGO. *Biosens. Bioelectron.* 126, 785–791
27. Yang, Y. *et al.* (2018) An ultrasensitive sandwich-type electrochemical immunosensor based on the signal amplification strategy of Echinoidea-shaped Au@Ag-Cu_2O nanoparticles for prostate specific antigen detection. *Biosens. Bioelectron.* 99, 450–457
28. Zhang, T. *et al.* (2019) The synergistic effect of Au-COF nanosheets and artificial peroxidase Au@ZIF-8(NiPd) rhombic dodecahedra for signal amplification for biomarker detection. *Nanoscale* 11, 20221–20227
29. Pakchin, P.S. *et al.* (2018) Electrochemical immunosensor based on chitosan-gold nanoparticle/carbon nanotube as a platform and lactate oxidase as a label for detection of CA125 oncomarker. *Biosens. Bioelectron.* 122, 68–74
30. Zhao, H. *et al.* (2021) Electrochemical immunosensor based on Au/Co-BDC/MoS_2 and DPCN/MoS_2 for the detection of cardiac troponin I. *Biosens. Bioelectron.* 175, 112883
31. Kim, S.H. *et al.* (2019) A new coccolith modified electrode-based biosensor using a cognate pair of aptamers with sandwich-type binding. *Biosens. Bioelectron.* 123, 160–166
32. Nguyen, T.T.-Q. *et al.* (2022) A new cognate aptamer pair-based sandwich-type electrochemical biosensor for sensitive detection of *Staphylococcus aureus*. *Biosens. Bioelectron.* 198, 113835
33. Joe, C. *et al.* (2022) Aptamer duo-based portable electrochemical biosensors for early diagnosis of periodontal disease. *Biosens. Bioelectron.* 199, 113884
34. Lv, H. *et al.* (2019) An electrochemical sandwich immunosensor for cardiac troponin I by using nitrogen/sulfur co-doped graphene oxide modified with Au@Ag nanocubes as amplifiers. *Microchim. Acta* 186, 416
35. Tang, Z. *et al.* (2018) A sensitive sandwich-type immunosensor for the detection of galectin-3 based on N-GNRs-Fe-MOFs@AuNPs nanocomposites and a novel AuPt-methylene blue nanorod. *Biosens. Bioelectron.* 101, 253–259
36. Chen, Y. *et al.* (2019) A sandwich-type electrochemical aptasensor for *Mycobacterium tuberculosis* MPT64 antigen detection using C60NPs decorated N-CNTs/GO nanocomposite coupled with conductive PEI-functionalized metal-organic framework. *Biomaterials* 216, 119253
37. Sun, D. *et al.* (2019) DNA nanotetrahedron-assisted electrochemical aptasensor for cardiac troponin I detection based on the co-catalysis of hybrid nanozyme, natural enzyme and artificial DNAzyme. *Biosens. Bioelectron.* 142, 111578
38. Zhang, T. *et al.* (2018) Electrochemical ultrasensitive detection of cardiac troponin I using covalent organic frameworks for signal amplification. *Biosens. Bioelectron.* 119, 176–181
39. Lv, S. *et al.* (2020) D. ZIF-8-assisted NaYF4:Yb,Tm@ZnO converter with exonuclease III-powered DNA walker for near-infrared light responsive biosensor. *Anal. Chem.* 92, 1470–1476
40. Kim, H. *et al.* (2018) A shape-code nanoplasmonic biosensor for multiplex detection of Alzheimer's disease biomarkers. *Biosens. Bioelectron.* 101, 96–102
41. Kim, H. *et al.* (2019) A nanoplasmonic biosensor for ultrasensitive detection of Alzheimer's disease biomarker using a chaotropic agent. *ACS Sens.* 4, 595–602
42. Wu, Q. *et al.* (2019) A 2D transition metal carbide MXene-based SPR biosensor for ultrasensitive carcinoembryonic antigen detection. *Biosens. Bioelectron.* 144, 111697
43. Chiavaioli, F. *et al.* (2018) Femtomolar detection by nanocoated fiber label-free biosensors. *ACS Sens.* 3, 936–943
44. Kaushik, S. *et al.* (2019) Two-dimensional transition metal dichalcogenides assisted biofunctionalized optical fiber SPR biosensor for efficient and rapid detection of bovine serum albumin. *Sci. Rep.* 9, 6987
45. Bekmurzayeva, A. *et al.* (2022) Ultra-wide, attomolar-level limit detection of CD44 biomarker with a silanized optical fiber biosensor. *Biosens. Bioelectron.* 208, 114217
46. Yazdanparast, S. *et al.* (2018) Dual-aptamer based electrochemical sandwich biosensor for MCF-7 human breast cancer cells using silver nanoparticle labels and a poly(glutamic acid)/MWNT nanocomposite. *Microchim. Acta* 185, 405
47. Tang, S. *et al.* (2018) A novel cytosensor based on Pt@Ag nanoflowers and AuNPs/acetylene black for ultrasensitive and highly specific detection of circulating tumor cells. *Biosens. Bioelectron.* 104, 72–78
48. Sun, D. *et al.* (2018) Competitive electrochemical platform for ultrasensitive cytosensing of liver cancer cells by using nanotetrahedra structure with rolling circle amplification. *Biosens. Bioelectron.* 120, 8–14
49. Shen, H. *et al.* (2020) Ultrasensitive aptasensor for isolation and detection of circulating tumor cells based on CeO_2@Ir nanorods and DNA walker. *Biosens. Bioelectron.* 168, 112516
50. Zhou, X. *et al.* (2019) A amperometric immunosensor for sensitive detection of circulating tumor cells using a tyramide signal amplification-based signal enhancement system. *Biosens. Bioelectron.* 130, 88–94

51. Cao, Y. *et al.* (2019) Integration of fluorescence imaging and electrochemical biosensing for both qualitative location and quantitative detection of cancer cells. *Biosens. Bioelectron.* 130, 132–138
52. Yang, J. *et al.* (2020) In situ-generated multivalent aptamer network for efficient capture and sensitive electrochemical detection of circulating tumor cells in whole blood. *Anal. Chem.* 92, 7893–7899
53. Dou, B. *et al.* (2019) Aptamer-functionalized and gold nanoparticle array-decorated magnetic graphene nanosheets enable multiplexed and sensitive electrochemical detection of rare circulating tumor cells in whole blood. *Anal. Chem.* 91, 10792–10799
54. Shen, C. *et al.* (2019) Electrochemical detection of circulating tumor cells based on DNA generated electrochemical current and rolling circle amplification. *Anal. Chem.* 91, 11614–11619
55. Luo, J. *et al.* (2020) Photoelectrochemical detection of circulating tumor cells based on aptamer conjugated Cu_2O as signal probe. *Biosens. Bioelectron.* 151, 111976
56. Wang, S.-S. *et al.* (2019) Direct plasmon-enhanced electrochemistry for enabling ultrasensitive and label-free detection of circulating tumor cells in blood. *Anal. Chem.* 91, 4413–4420
57. Loyez, M. *et al.* (2020) Rapid detection of circulating breast cancer cells using a multiresonant optical fiber aptasensor with plasmonic amplification. *ACS Sens.* 5, 454–463
58. Paterlini-Brechot, P. and Benali, N.L. (2007) Circulating tumor cells (CTC) detection: clinical impact and future directions. *Cancer Lett.* 253, 180–204
59. Amerongen, A. van *et al.* (2018) Lateral flow immunoassays. In *Handbook of Immunoassay Technologies* (Vashist, S.K. and Luong, J.H.T., eds), pp. 157–182, Academic Press
60. Raston, N.H.A. *et al.* (2017) A new lateral flow strip assay (LFSA) using a pair of aptamers for the detection of Vaspin. *Biosens. Bioelectron.* 93, 21–25
61. Kim, S.H. *et al.* (2019) Specific detection of avian influenza H5N2 whole virus particles on lateral flow strips using a pair of sandwich-type aptamers. *Biosens. Bioelectron.* 134, 123–129
62. Lee, B.H. *et al.* (2019) The sensitive detection of ODAM by using sandwich-type biosensors with a cognate pair of aptamers for the early diagnosis of periodontal disease. *Biosens. Bioelectron.* 126, 122–128
63. Sena-Torralba, A. *et al.* (2020) Lateral flow assay modified with time-delay wax barriers as a sensitivity and signal enhancement strategy. *Biosens. Bioelectron.* 168, 112559
64. Loynachan, C.N. *et al.* (2018) Platinum nanocatalyst amplification: redefining the gold standard for lateral flow immunoassays with ultrabroad dynamic range. *ACS Nano* 12, 279–288
65. Wang, J. *et al.* (2021) Ratiometric fluorescent lateral flow immunoassay for point-of-care testing of acute myocardial infarction. *Angew. Chem. Int. Ed.* 60, 13042–13049
66. Miller, B.S. *et al.* (2020) Spin-enhanced nanodiamond biosensing for ultrasensitive diagnostics. *Nature* 587, 588–593
67. Deng, X. *et al.* (2018) Applying strand displacement amplification to quantum dots-based fluorescent lateral flow assay strips for HIV-DNA detection. *Biosens. Bioelectron.* 105, 211–217
68. Tran, V. *et al.* (2019) Rapid, quantitative, and ultrasensitive point-of-care testing: a portable SERS reader for lateral flow assays in clinical chemistry. *Angew. Chem. Int. Ed.* 58, 442–446
69. Wang, C. *et al.* (2019) Magnetic SERS strip for sensitive and simultaneous detection of respiratory viruses. *ACS Appl. Mater. Inter.* 11, 19495–19505
70. Zhang, D. *et al.* (2018) Quantitative and ultrasensitive detection of multiplex cardiac biomarkers in lateral flow assay with core-shell SERS nanotags. *Biosens. Bioelectron.* 106, 204–211
71. Rivas, L. *et al.* (2014) Improving sensitivity of gold nanoparticle-based lateral flow assays by using wax-printed pillars as delay barriers of microfluidics. *Lab Chip* 14, 4406–4414
72. Preechakasedkit, P. *et al.* (2018) Development of an automated wax-printed paper-based lateral flow device for alpha-fetoprotein enzyme-linked immunosorbent assay. *Biosens. Bioelectron.* 102, 27–32
73. Choi, J.R. *et al.* (2017) Lateral flow assay based on paper–hydrogel hybrid material for sensitive point-of-care detection of Dengue virus. *Adv. Healthc. Mater.* 6, 1600920
74. Kim, W. *et al.* (2018) Enhanced sensitivity of lateral flow immunoassays by using water-soluble nanofibers and silver-enhancement reactions. *Sens. Actuators B Chem.* 273, 1323–1327
75. Han, G.-R. *et al.* (2020) Paper/soluble polymer hybrid-based lateral flow biosensing platform for high-performance point-of-care testing. *ACS Appl. Mater. Interfaces* 12, 34564–34575
76. Brangel, P. *et al.* (2018) A serological point-of-care test for the detection of IgG antibodies against Ebola virus in human survivors. *ACS Nano* 12, 63–73
77. Funari, R. *et al.* (2020) Detection of antibodies against SARS-CoV-2 spike protein by gold nanospikes in an opto-microfluidic chip. *Biosens. Bioelectron.* 169, 112578
78. Najjar, D. *et al.* (2022) A lab-on-a-chip for the concurrent electrochemical detection of SARS-CoV-2 RNA and anti-SARS-CoV-2 antibodies in saliva and plasma. *Nat. Biomed. Eng.* 6, 968–978
79. Ali, Md.A. *et al.* (2021) Sensing of COVID-19 antibodies in seconds via aerosol jet nanoprinted reduced-graphene-oxide-coated 3D electrodes. *Adv. Mater.* 33, 2006647
80. Chen, C.-A. *et al.* (2019) Three-dimensional origami paper-based device for portable immunoassay applications. *Lab Chip* 19, 598–607
81. Jiao, Y. *et al.* (2020) 3D vertical-flow paper-based device for simultaneous detection of multiple cancer biomarkers by fluorescent immunoassay. *Sens. Actuators B Chem.* 306, 127239
82. Verma, M.S. *et al.* (2018) Sliding-strip microfluidic device enables ELISA on paper. *Biosens. Bioelectron.* 99, 77–84
83. Reboud, J. *et al.* (2019) Paper-based microfluidics for DNA diagnostics of malaria in low resource underserved rural communities. *Proc. Natl. Acad. Sci. U. S. A.* 116, 4834–4842
84. Wei, B. *et al.* (2018) Graphene nanocomposites modified electrochemical aptamer sensor for rapid and highly sensitive detection of prostate specific antigen. *Biosens. Bioelectron.* 121, 41–46
85. Bhardwaj, J. *et al.* (2019) Vertical flow-based paper immunosensor for rapid electrochemical and colorimetric detection of influenza virus using a different pore size sample pad. *Biosens. Bioelectron.* 126, 36–43
86. Sun, X. *et al.* (2018) Ultrasensitive microfluidic paper-based electrochemical/visual biosensor based on spherical-like cerium dioxide catalyst for miR-21 detection. *Biosens. Bioelectron.* 105, 218–222
87. Yakoh, A. *et al.* (2019) 3D capillary-driven paper-based sequential microfluidic device for electrochemical sensing applications. *ACS Sens.* 4, 1211–1221
88. Boonkaew, S. *et al.* (2021) An automated fast-flow/delayed paper-based platform for the simultaneous electrochemical detection of hepatitis B virus and hepatitis C virus core antigen. *Biosens. Bioelectron.* 193, 113543
89. Yakoh, A. *et al.* (2021) Paper-based electrochemical biosensor for diagnosing COVID-19: detection of SARS-CoV-2 antibodies and antigen. *Biosens. Bioelectron.* 176, 112912
90. Wang, Y. *et al.* (2019) Label-free microfluidic paper-based electrochemical aptasensor for ultrasensitive and simultaneous multiplexed detection of cancer biomarkers. *Biosens. Bioelectron.* 136, 84–90
91. Qi, J. *et al.* (2019) The strategy of antibody-free biomarker analysis by in-situ synthesized molecularly imprinted polymers on movable valve paper-based device. *Biosens. Bioelectron.* 142, 111533
92. Martinez, A.W. *et al.* (2007) Patterned paper as a platform for inexpensive, low-volume, portable bioassays. *Angew. Chem. Int. Ed.* 46, 1318–1320
93. Dungchai, W. *et al.* (2009) Electrochemical detection for paper-based microfluidics. *Anal. Chem.* 81, 5821–5826
94. Pardee, K. *et al.* (2016) Rapid, low-cost detection of Zika virus using programmable biomolecular components. *Cell* 165, 1255–1266
95. Broughton, J.P. *et al.* (2020) CRISPR–Cas12-based detection of SARS-CoV-2. *Nat. Biotechnol.* 38, 870–874
96. Wang, X. *et al.* (2020) Clustered regularly interspaced short palindromic repeats/cas9-mediated lateral flow nucleic acid assay. *ACS Nano* 14, 2497–2508
97. Gootenberg, J.S. *et al.* (2018) Multiplexed and portable nucleic acid detection platform with Cas13, Cas12a, and Csm6. *Science* 360, 439–444

98. Bruch, R. *et al.* (2019) CRISPR/Cas13a-powered electrochemical microfluidic biosensor for nucleic acid amplification-free miRNA diagnostics. *Adv. Mater.* 31, 1905311
99. Bruch, R. *et al.* (2021) CRISPR-powered electrochemical microfluidic multiplexed biosensor for target amplification-free miRNA diagnostics. *Biosens. Bioelectron.* 177, 112887
100. Chen, Q. *et al.* (2020) CRISPR/Cas13a signal amplification linked immunosorbent assay for femtomolar protein detection. *Anal. Chem.* 92, 573–577
101. Zhao, Q. *et al.* (2021) Nano-immunosorbent assay based on Cas12a/crRNA for ultra-sensitive protein detection. *Biosens. Bioelectron.* 190, 113450
102. Lin, X. *et al.* (2022) CRISPR-Cas12a-mediated luminescence resonance energy transfer aptasensing platform for deoxynivalenol using gold nanoparticle-decorated Ti3C2Tx MXene as the enhanced quencher. *J. Hazard. Mater.* 433, 128750
103. Niu, C. *et al.* (2021) Aptamer assisted CRISPR-Cas12a strategy for small molecule diagnostics. *Biosens. Bioelectron.* 183, 113196
104. Xiong, Y. *et al.* (2020) Functional DNA regulated CRISPR-Cas12a sensors for point-of-care diagnostics of non-nucleic-acid targets. *J. Am. Chem. Soc.* 142, 207–213
105. Zhao, X. *et al.* (2021) A versatile biosensing platform coupling CRISPR–Cas12a and aptamers for detection of diverse analytes. *Sci. Bull.* 66, 69–77
106. Li, C.-Y. *et al.* (2021) Holographic optical tweezers and boosting upconversion luminescent resonance energy transfer combined clustered regularly interspaced short palindromic repeats (CRISPR)/Cas12a biosensors. *ACS Nano* 15, 8142–8154
107. Dai, Y. *et al.* (2019) Exploring the trans-cleavage activity of CRISPR-Cas12a (cpf1) for the development of a universal electrochemical biosensor. *Angew. Chem. Int. Ed.* 58, 17399–17405
108. Mei-Ling, L. *et al.* (2022) Y-shaped DNA nanostructures assembled-spherical nucleic acids as target converters to activate CRISPR-Cas12a enabling sensitive ECL biosensing. *Biosens. Bioelectron.* 214, 114512
109. Yuan, G. *et al.* (2022) A novel 'signal on-off-super on' sandwich-type aptamer sensor of CRISPR-Cas12a coupled voltage enrichment assay for VEGF detection. *Biosens. Bioelectron.* 114424
110. Iwasaki, R.S. and Batey, R.T. (2020) SPRINT: a Cas13a-based platform for detection of small molecules. *Nucleic Acids Res.* 48, e101
111. Liang, M. *et al.* (2019) A CRISPR-Cas12a-derived biosensing platform for the highly sensitive detection of diverse small molecules. *Nat. Commun.* 10, 3672
112. Mastrototaro, J.J. (2000) The MiniMed continuous glucose monitoring system. *Diabetes Technol. Ther.* 2, 13–18
113. Valdés-Ramírez, G. *et al.* (2014) Microneedle-based self-powered glucose sensor. *Electrochem. Commun.* 47, 58–62
114. Heifler, O. *et al.* (2021) Clinic-on-a-needle array toward future minimally invasive wearable artificial pancreas applications. *ACS Nano* 15, 12019–12033
115. Lipani, L. *et al.* (2018) Non-invasive, transdermal, path-selective and specific glucose monitoring via a graphene-based platform. *Nat. Nanotechnol.* 13, 504–511
116. Kim, J. *et al.* (2018) Simultaneous monitoring of sweat and interstitial fluid using a single wearable biosensor platform. *Adv. Sci.* 5, 1800880
117. Shibata, H. *et al.* (2010) Injectable hydrogel microbeads for fluorescence- based in vivo continuous glucose monitoring. *Proc. Natl. Acad. Sci. U. S. A.* 107, 17894–17898
118. Kropff, J. *et al.* (2016) Accuracy and longevity of an implantable continuous glucose sensor in the PRECISE study: a 180-day, prospective, multicenter, pivotal trial. *Diabetes Care* 40, 63–68
119. Goud, K.Y. *et al.* (2019) Wearable electrochemical microneedle sensor for continuous monitoring of levodopa: toward Parkinson management. *ACS Sens.* 4, 2196–2204
120. Gowers, S.A.N. *et al.* (2019) Development of a minimally invasive microneedle-based sensor for continuous monitoring of β-lactam antibiotic concentrations in vivo. *Acs Sens.* 4, 1072–1080
121. Swensen, J.S. *et al.* (2009) Continuous, real-time monitoring of cocaine in undiluted blood serum via a microfluidic, electrochemical aptamer-based sensor. *J. Am. Chem. Soc.* 131, 4262–4266
122. Kurnik, M. *et al.* (2020) An electrochemical biosensor architecture based on protein folding supports direct real-time measurements in whole blood. *Angew. Chem. Int. Ed.* 59, 18442–18445
123. Ferguson, B.S. *et al.* (2013) Real-Time, aptamer-based tracking of circulating therapeutic agents in living animals. *Sci. Transl. Med.* 5, 213ra165
124. Arroyo-Currás, N. *et al.* (2017) Real-time measurement of small molecules directly in awake, ambulatory animals. *Proc. Natl. Acad. Sci. U. S. A.* 114, 645–650
125. Dauphin-Ducharme, P. *et al.* (2019) Electrochemical aptamer-based sensors for improved therapeutic drug monitoring and high-precision, feedback-controlled drug delivery. *ACS Sens.* 4, 2832–2837
126. Wu, Y. *et al.* (2022) Microneedle aptamer-based sensors for continuous, real-time therapeutic drug monitoring. *Anal. Chem.* 94, 8335–8345
127. Poudineh, M. *et al.* (2021) A fluorescence sandwich immunoassay for the real-time continuous detection of glucose and insulin in live animals. *Nat. Biomed. Eng.* 5, 53–63
128. Mohan, A.M.V. *et al.* (2017) Continuous minimally-invasive alcohol monitoring using microneedle sensor arrays. *Biosens. Bioelectron.* 91, 574–579
129. Tehrani, F. *et al.* (2022) An integrated wearable microneedle array for the continuous monitoring of multiple biomarkers in interstitial fluid. *Nat. Biomed. Eng.* 1–11
130. Ciui, B. *et al.* (2018) Wearable wireless tyrosinase bandage and microneedle sensors: toward melanoma screening. *Adv. Healthc. Mater.* 7, 1701264
131. Bao, L. *et al.* (2022) Anti-SARS-CoV-2 IgM/IgG antibodies detection using a patch sensor containing porous microneedles and a paper-based immunoassay. *Sci. Rep.* 12, 10693
132. Arakawa, T. *et al.* (2020) A wearable cellulose acetate-coated mouthguard biosensor for in vivo salivary glucose measurement. *Anal. Chem.* 92, 12201–12207
133. Tseng, P. *et al.* (2018) RF-trilayer sensors for tooth-mounted, wireless monitoring of the oral cavity and food consumption. *Adv. Mater.* 30, 1703257
134. Kim, J. *et al.* (2017) Wearable smart sensor systems integrated on soft contact lenses for wireless ocular diagnostics. *Nat. Commun.* 8, 14997
135. Park, J. *et al.* (2018) Soft, smart contact lenses with integrations of wireless circuits, glucose sensors, and displays. *Sci. Adv.* 4, eaap9841
136. Song, H. *et al.* (2022) Wireless non-invasive monitoring of cholesterol using a smart contact lens. *Adv. Sci.* 9, 2203597
137. Elsherif, M. *et al.* (2018) Wearable contact lens biosensors for continuous glucose monitoring using smartphones. *ACS Nano* 12, 5452–5462
138. Ye, Y. *et al.* (2022) Smart contact lens with dual-sensing platform for monitoring intraocular pressure and matrix metalloproteinase-9. *Adv. Sci.* 9, 2104738
139. Sempionatto, J.R. *et al.* (2019) Eyeglasses-based tear biosensing system: non-invasive detection of alcohol, vitamins and glucose. *Biosens. Bioelectron.* 137, 161–170
140. Bandodkar, A.J. *et al.* (2015) Tattoo-based noninvasive glucose monitoring: a proof-of-concept study. *Anal. Chem.* 87, 394–398
141. Gao, W. *et al.* (2016) Fully integrated wearable sensor arrays for multiplexed in situ perspiration analysis. *Nature* 529, 509–514
142. Sempionatto, J.R. *et al.* (2021) An epidermal patch for the simultaneous monitoring of haemodynamic and metabolic biomarkers. *Nat. Biomed. Eng.* 5, 737–748
143. Chen, Y. *et al.* (2017) Skin-like biosensor system via electrochemical channels for noninvasive blood glucose monitoring. *Sci. Adv.* 3, e1701629
144. Kim, Y. *et al.* (2022) Chip-less wireless electronic skins by remote epitaxial freestanding compound semiconductors. *Science* 377, 859–864
145. Koh, A. *et al.* (2016) A soft, wearable microfluidic device for the capture, storage, and colorimetric sensing of sweat. *Sci. Transl. Med.* 8, 366ra165
146. Bandodkar, A.J. *et al.* (2019) Battery-free, skin-interfaced microfluidic/electronic systems for simultaneous electrochemical, colorimetric, and volumetric analysis of sweat. *Sci. Adv.* 5, eaav3294

147. Kim, S. *et al.* (2020) Soft, skin-interfaced microfluidic systems with integrated immunoassays, fluorometric sensors, and impedance measurement capabilities. *Proc. Natl. Acad. Sci. U. S. A.* 117, 27906–27915
148. Lee, H.-B. *et al.* (2020) A wearable lab-on-a-patch platform with stretchable nanostructured biosensor for non-invasive immunodetectzzzzion of biomarker in sweat. *Biosens. Bioelectron.* 156, 112133
149. Cheng, C. *et al.* (2021) Battery-free, wireless, and flexible electrochemical patch for in situ analysis of sweat cortisol via near field communication. *Biosens. Bioelectron.* 172, 112782
150. Wang, B. *et al.* (2022) Wearable aptamer-field-effect transistor sensing system for noninvasive cortisol monitoring. *Sci. Adv.* 8, eabk0967
151. An, J.E. *et al.* (2022) Wearable cortisol aptasensor for simple and rapid real-time monitoring. *ACS Sens.* 7, 99–108
152. Wang, Z. *et al.* (2021) A flexible and regenerative aptameric graphene–nafion biosensor for cytokine storm biomarker monitoring in undiluted biofluids toward wearable applications. *Adv. Funct. Mater.* 31, 2005958
153. Liu, T.-L. *et al.* (2022) Battery-free, tuning circuit-inspired wireless sensor systems for detection of multiple biomarkers in bodily fluids. *Sci. Adv.* 8, eabo7049
154. Gonzalez-Navarro, F.F. *et al.* (2016) Glucose oxidase biosensor modeling and predictors optimization by machine learning methods. *Sensors* 16, 1483
155. Yan, W. *et al.* (2019) Machine learning approach to enhance the performance of MNP-labeled lateral flow immunoassay. *Nano-micro Lett.* 11, 7
156. Massah, J. and Vakilian, K.A. (2019) An intelligent portable biosensor for fast and accurate nitrate determination using cyclic voltammetry. *Biosyst. Eng.* 177, 49–58